A Mass-Lumped Mixed Finite Element Method for Maxwell's Equations

Herbert Egger and Bogdan Radu

Abstract A novel mass-lumping strategy for a mixed finite element approximation of Maxwell's equations is proposed which on structured orthogonal grids coincides with the spatial discretization of the Yee scheme. The proposed method, however, generalizes naturally to unstructured grids and anisotropic materials and thus yields a natural variational extension of the Yee scheme for these situations.

1 Introduction

We consider the propagation of electromagnetic radiation through a linear non-dispersive and non-conducting medium described by Maxwell's equations

$$\epsilon \partial_t \mathbf{E} = \operatorname{curl} \mathbf{H}, \tag{1}$$

$$\mu \partial_t \mathbf{H} = -\operatorname{curl} \mathbf{E}. \tag{2}$$

Here $\mathbf{E}$, $\mathbf{H}$ denote the electric and magnetic field intensities and ϵ, μ are the symmetric and positive definite permittivity and permeability tensors. For ease of notation, we assume that $\mathbf{E} \times \mathbf{n} = 0$ on the boundary. The space discretization of (1)–(2) usually leads to finite dimensional differential equations of the form

$$\mathrm{M}_\epsilon \partial_t \mathbf{e} = \mathrm{C}' \mathbf{h}, \tag{3}$$

$$\mathrm{M}_\mu \partial_t \mathbf{h} = -\mathrm{C}\mathbf{e}. \tag{4}$$

H. Egger (✉)
Department of Mathematics, TU Darmstadt, Darmstadt, Germany
e-mail: egger@mathematik.tu-darmstadt.de

B. Radu
Graduate School for Computational Engineering, TU Darmstadt, Darmstadt, Germany
e-mail: radu@gsc.tu-darmstadt.de

G. Nicosia, V. Romano (eds.), *Scientific Computing in Electrical Engineering*,
Mathematics in Industry 32, https://doi.org/10.1007/978-3-030-44101-2_2

Due to the particular structure of the system, the stability of such discretization schemes can easily be ensured by the simple algebraic conditions

(i) $\mathrm{C}' = \mathrm{C}^\top$,
(ii) $\mathrm{M}_\epsilon, \mathrm{M}_\mu$ symmetric and positive definite.

In order to enable an efficient solution of (3)–(4) by explicit time-stepping methods, one additionally has to assume that

(iii) $\mathrm{M}_\epsilon^{-1}, \mathrm{M}_\mu^{-1}$ can be applied efficiently.

The finite difference approximation of (1)–(2) on staggered orthogonal grids yields approximations of the form (3)–(4) satisfying the conditions (i)–(iii) with diagonal matrices M_ϵ, M_μ [13]. Moreover, the entries $\mathbf{e}_i$, $\mathbf{h}_j$ in the solution vectors yield second order approximations for the line integrals of $\mathbf{E}$, $\mathbf{H}$ along edges of the primal and dual grids [3, 12]. An extension to unstructured grids and anisotropic coefficients is in principle possible, but these approaches rely on the use of two sets of unstructured grids [2, 11] which makes a rigorous convergence analysis rather difficult.

The finite element approximation of (1)–(2) on the other hand yields systems of the form (3)–(4) satisfying conditions (i)–(ii) automatically and a rigorous convergence analysis is possible in rather general situations [7–9]. Although the matrices M_ϵ and M_μ are usually sparse, condition (iii) is here in general not valid. The resulting lack of efficiency can however be overcome by appropriate *mass-lumping* [4, 6], which aims at approximating M_ϵ and M_μ by diagonal or block-diagonal matrices. These approaches are usually based on an enrichment of the approximation spaces and appropriate quadrature; see [3] for details and further references.

In this paper, we present a novel mass-lumping strategy for a mixed finite element approximation of (1)–(2) that yields properties (i)–(iii) without such an increase of the system dimension. We further show that in special cases, i.e., for orthogonal grids and scalar coefficients, the resulting scheme reduces to the staggered-grid finite difference approximation of the Yee scheme.

2 A Mass-Lumped Mixed Finite Element Method

As a preliminary step, we consider a mass-lumped mixed finite element approximation based on enriched approximation spaces and numerical quadrature. We seek for approximations $\widetilde{\mathbf{E}}_h(t) \in \widetilde{V}_h$, $\widetilde{\mathbf{H}}_h(t) \in \widetilde{Q}_h$ satisfying

$$(\epsilon \partial_t \widetilde{\mathbf{E}}_h(t), \widetilde{\mathbf{v}}_h)_h = (\widetilde{\mathbf{H}}_h(t), \operatorname{curl} \widetilde{\mathbf{v}}_h) \qquad \forall \widetilde{\mathbf{v}}_h \in \widetilde{V}_h, \tag{5}$$

$$(\mu \partial_t \widetilde{\mathbf{H}}_h(t), \widetilde{\mathbf{q}}_h)_{h,*} = -(\operatorname{curl} \widetilde{\mathbf{E}}_h(t), \widetilde{\mathbf{q}}_h) \qquad \forall \widetilde{\mathbf{q}}_h \in \widetilde{Q}_h, \tag{6}$$

for all $t > 0$. Here, $\widetilde{V}_h \subset H_0(\mathrm{curl};\Omega)$ and $\widetilde{Q}_h \subset L^2(\Omega)$ are appropriate finite dimensional subspaces and $(\mathbf{a},\mathbf{b})_h$, $(\mathbf{a},\mathbf{b})_{h,*}$ are approximations for usual the scalar product $(\mathbf{a},\mathbf{b}) = \int_\Omega \mathbf{a}(x)\cdot\mathbf{b}(x)\,dx$ to be defined below.

In the sequel, we restrict our discussion to problems where $\mathbf{E} = (E_x, E_y, 0)$ and $\mathbf{H} = (0, 0, H_z)$ with E_x, E_y, H_z independent of z, which allows to represent the fields in two dimensions. The extension to three dimensions will be discussed in Sect. 5.

Let $\mathcal{T}_h = \{T\}$ be a conforming mesh of Ω consisting of triangles and parallelograms. Any element $T \in \mathcal{T}_h$ is the image $F_T(\widehat{T})$ of a reference triangle or reference square under an affine mapping $F_T(\widehat{x}) = a_T + B_T\widehat{x}$ with $a_T \in \mathbb{R}^2$ and $B_T \in \mathbb{R}^{2\times 2}$. We denote by h the maximal element diameter and assume uniform shape regularity.

To every element T_j, $j = 1,\dots,n_T$ of the mesh, we associate one basis function $\widetilde{\psi}_j$ of the space $\widetilde{Q}_h$ with $\widetilde{\psi}_j|_{T_k} = \delta_{jk}$. For every interior edge $e_i = T_l \cap T_r$, $i = 1,\dots,n_e$ of the mesh, we further define two basis functions $\widetilde{\phi}_i, \widetilde{\phi}_{i+n_e}$ which are defined by

$$\widetilde{\phi}_{i+\ell\cdot n_e}|_T = B_T^{-\top}\widehat{\phi}_{\alpha,\gamma}, \qquad \ell = 0, 1, \tag{7}$$

on $T \in \{T_l, T_r\}$ and vanish identically on all other elements. Here $\alpha \in \{1,\dots,\widehat{n}_e\}$ refers to the number of the edge e_i on the reference element $\widehat{T}$ and $\gamma \in \{0, 1\}$ depends on ℓ and the orientation of the edge e_i. The functions $\widehat{\phi}_{\alpha,\gamma}$ are defined in Fig. 1. Similar approximation spaces in three dimensions were utilized in [8, 9]. We further set $(\mathbf{a},\mathbf{b})_{h,*} = (\mathbf{a},\mathbf{b})$ and define $(\mathbf{a},\mathbf{b})_h = \sum_T (\mathbf{a},\mathbf{b})_{h,T}$ with

$$(\mathbf{a},\mathbf{b})_{h,T} = |T| \sum_{l=1}^{\widehat{n}_p} \mathbf{a}(F_T(\widehat{x}_l))\cdot\mathbf{b}(F_T(\widehat{x}_l))\; w_l, \tag{8}$$

where $w_l = 1/\widehat{n}_p$ denote the quadrature weights and $\widehat{x}_l$, $l = 1,\dots,\widehat{n}_p$ the quadrature points on the reference element, depicted by dots in Fig. 1.

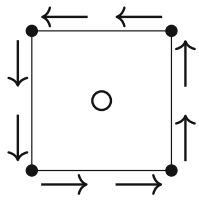

$\widehat{\phi}_{1,0} = \frac{1}{2}\begin{pmatrix}-y^2+y\\-2xy+2x\end{pmatrix}$, $\widehat{\phi}_{1,1} = \frac{1}{2}\begin{pmatrix}y^2-y\\2xy\end{pmatrix}$,
$\widehat{\phi}_{2,0} = \frac{1}{2}\begin{pmatrix}-2xy\\-x^2+x\end{pmatrix}$, $\widehat{\phi}_{2,1} = \frac{1}{2}\begin{pmatrix}-2y+2xy\\x^2-x\end{pmatrix}$,
$\widehat{\phi}_{3,0} = \frac{1}{2}\begin{pmatrix}y^2-y\\2xy-2y\end{pmatrix}$, $\widehat{\phi}_{3,1} = \frac{1}{2}\begin{pmatrix}-y^2+y\\2x+2y-2xy-2\end{pmatrix}$,
$\widehat{\phi}_{4,0} = \frac{1}{2}\begin{pmatrix}-2x-2y+2xy+2\\x^2-x\end{pmatrix}$, $\widehat{\phi}_{4,1} = \frac{1}{2}\begin{pmatrix}-2xy+2x\\-x^2+x\end{pmatrix}$.

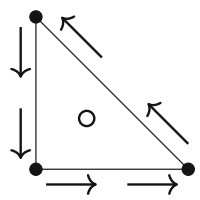

$\widehat{\phi}_{1,0} = \frac{1}{2}\begin{pmatrix}0\\x\end{pmatrix}$, $\widehat{\phi}_{1,1} = \frac{1}{2}\begin{pmatrix}-y\\0\end{pmatrix}$,
$\widehat{\phi}_{2,0} = \frac{1}{2}\begin{pmatrix}-y\\-y\end{pmatrix}$, $\widehat{\phi}_{2,1} = \frac{1}{2}\begin{pmatrix}0\\x+y-1\end{pmatrix}$,
$\widehat{\phi}_{3,0} = \frac{1}{2}\begin{pmatrix}1-x-y\\0\end{pmatrix}$, $\widehat{\phi}_{3,1} = \frac{1}{2}\begin{pmatrix}x\\x\end{pmatrix}$.

Fig. 1 Degrees of freedom and basis functions for the unit triangle and unit square. The black dots at the vertices represent the quadrature points for the quadrature formula introduced below

Using the bases defined above, all functions in $\widetilde{V}_h$ and $\widetilde{Q}_h$ can be represented as

$$\widetilde{\mathbf{E}}_h = \sum\nolimits_i \widetilde{\mathbf{e}}_i \widetilde{\phi}_i + \widetilde{\mathbf{e}}_{i+n_e} \widetilde{\phi}_{i+n_e} \qquad \text{and} \qquad \widetilde{\mathbf{H}}_h = \sum\nolimits_j \widetilde{\mathbf{h}}_j \widetilde{\psi}_j. \tag{9}$$

This allows to rewrite the variational problem (5)–(6) in algebraic form as

$$\widetilde{\mathrm{M}}_\epsilon \partial_t \widetilde{\mathbf{e}} = \widetilde{\mathrm{C}}^\top \widetilde{\mathbf{h}}, \tag{10}$$

$$\widetilde{\mathrm{M}}_\mu \partial_t \widetilde{\mathbf{h}} = -\widetilde{\mathrm{C}} \widetilde{\mathbf{e}}, \tag{11}$$

with matrices $(\widetilde{\mathrm{M}}_\epsilon)_{ij} = (\epsilon \widetilde{\phi}_j, \widetilde{\phi}_i)_h$, $(\widetilde{\mathrm{M}}_\mu)_{ij} = (\mu \widetilde{\psi}_j, \widetilde{\psi}_i)$, and $(\widetilde{\mathrm{C}})_{ij} = (\mathrm{curl}\, \widetilde{\phi}_j, \widetilde{\psi}_i)$. As a direct consequence of the particular choice of the basis functions, we obtain

Lemma 1 *Let $\widetilde{\mathrm{M}}_\epsilon$, $\widetilde{\mathrm{M}}_\mu$, and $\widetilde{\mathrm{C}}$ be defined as above. Then conditions (i)–(iii) hold.*

Proof The properties (i)–(ii) follow directly from the definition of the matrices and the symmetric positive definiteness of the material tensors. Since the basis functions for $\widetilde{Q}_h$ are supported only on single elements, one can see that $\widetilde{\mathrm{M}}_\mu$ is diagonal. To see the block-diagonal structure of $\widetilde{\mathrm{M}}_\epsilon$, let us refer to Fig. 2. In the left plot, the degrees of freedom for $\widetilde{V}_h$ are depicted by the red arrows and the quadrature points by blue circles. By definition, the corresponding basis functions are zero in all vertices, except the one which the arrow representing the corresponding degree of freedom originates from. Together with the nodal quadrature formula, this reveals that only groups of basis functions associated with same vertex yield non-zero contributions to the mass matrix $\widetilde{\mathrm{M}}_\epsilon$. In the right plot of Fig. 2, we depict the structure of the inverse of $\widetilde{\mathrm{M}}_\epsilon^{-1}$. Each block here corresponds to the degrees of freedom associated to one of the vertices in the mesh and the size of the block is determined by the number of edges incident to the corresponding vertex. Note

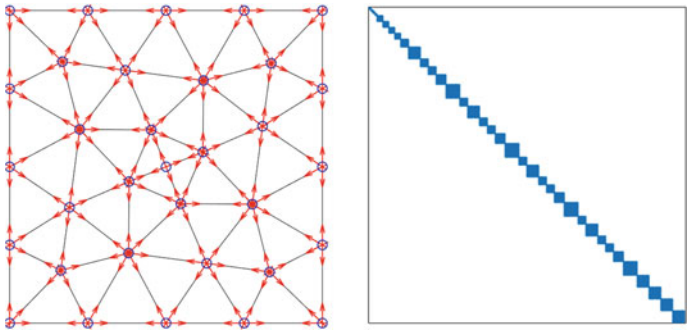

Fig. 2 Location of degrees of freedom for the basis function of the space $\widetilde{V}_h$ (left), and structure of the matrix $\widetilde{\mathrm{M}}_\epsilon^{-1}$ after appropriate numbering of degrees of freedom (right)

that an appropriate numbering of the degrees of freedom is required to see the block diagonal structure so clearly. □

Let us mention that the quadrature rule satisfies $(\mathbf{a}, \mathbf{b})_{h,T} = \int_T \mathbf{a}(x) \cdot \mathbf{b}(x)\, dx$ when $\mathbf{a}(x) \cdot \mathbf{b}(x)$ is affine linear. This ensures that the method (5)–(6) also has good approximation properties. By a slight adoption of the results given in [5], we obtain

Lemma 2 *Let* $\mathbf{E}$, $\mathbf{H}$ *be a smooth solution of (1)–(2) and let* $\widetilde{\mathbf{E}}_h(0)$ *and* $\widetilde{\mathbf{H}}_h(0)$ *be chosen appropriately. Then*

$$\|\widetilde{\mathbf{E}}_h(t) - \mathbf{E}(t)\|_{L^2(\Omega)} + \|\widetilde{\mathbf{H}}_h(t) - \mathbf{H}(t)\|_{L^2(\Omega)} \le Ch,$$

for all $0 \le t \le T$ *with* $C = C(\mathbf{E}, \mathbf{H}, T)$. *Moreover,* $\|\widetilde{\mathbf{H}}_h(t) - \pi_h^0 \mathbf{H}(t)\|_{L^2(\Omega)} \le Ch^2$ *where* $\pi_h^0 \mathbf{H}$ *denotes the piecewise constant approximation of* $\mathbf{H}$ *on the mesh* $\mathcal{T}_h$.

Remark 1 For structured meshes and isotropic coefficients, one can observe second order convergence also for line integrals of the electric field along edges of the mesh. Second convergence for the electric field can also be obtained for unstructured meshes by a non-local post-processing strategy; see [5] for details.

3 A Variational Extension of the Yee Scheme

The method of the previous section already yields a stable and efficient approximation. We now show that one degree of freedom per edge can be saved without sacrificing the accuracy or efficiency of the method. To this end, we construct approximations $\mathbf{E}_h(t) \in V_h$, $\mathbf{H}_h(t) \in Q_h$ in spaces $V_h \subset \widetilde{V}_h$ and $Q_h = \widetilde{Q}_h$.

We again define one basis function ψ_j of Q_h for every element T_k by $\psi_j|_{T_k} = \delta_{jk}$. To any edge $e_i = T_l \cap T_r$, we now associate one single basis function ϕ_i defined by

$$\phi_i = \widetilde{\phi}_i + \widetilde{\phi}_{i+n_e}. \tag{12}$$

Using the construction of $\widetilde{\phi}_i$, one can give an equivalent definition of ϕ_i via

$$\phi_i|_T = B_T^{-\top} \widehat{\phi}_\alpha, \qquad T \cap e_i \neq \emptyset, \tag{13}$$

with basis functions $\widehat{\phi}_\alpha = \widehat{\phi}_{\alpha,0} + \widehat{\phi}_{\alpha,1}$ defined on the reference element in Fig. 3. Note that the space V_h coincides with the Nedelec space of lowest order [1, 10]. Any function $\mathbf{E}_h \in V_h$ and $\mathbf{H}_h \in Q_h$ can now be expanded as

$$\mathbf{E}_h = \sum\nolimits_i \mathbf{e}_i \phi_i \qquad \text{and} \qquad \mathbf{H}_h = \sum\nolimits_j \mathbf{h}_j \psi_j. \tag{14}$$

$\widehat{\phi}_1 = \binom{0}{x}, \quad \widehat{\phi}_2 = \binom{-y}{0},$
$\widehat{\phi}_3 = \binom{0}{x-1}, \quad \widehat{\phi}_4 = \binom{1-y}{0}.$

$\widehat{\phi}_1 = \frac{1}{2}\binom{-y}{x}, \quad \widehat{\phi}_2 = \frac{1}{2}\binom{-y}{x-1}$
$\widehat{\phi}_3 = \frac{1}{2}\binom{1-y}{x}.$

Fig. 3 Degrees of freedom and basis functions on the unit triangle and unit square

As a consequence of (12), any $\mathbf{E}_h \in V_h$ can be interpreted as function $\widetilde{\mathbf{E}}_h \in \widetilde{V}_h$ by

$$\mathbf{E}_h = \sum\nolimits_i \mathbf{e}_i \phi_i = \sum\nolimits_i \mathbf{e}_i (\widetilde{\phi}_i + \widetilde{\phi}_{i+n_e}) = \sum\nolimits_i \mathbf{e}_i \widetilde{\phi}_i + \mathbf{e}_i \widetilde{\phi}_{i+n_e} = \widetilde{\mathbf{E}}_h. \tag{15}$$

The coordinates of $\widetilde{\mathbf{E}}_h$ and $\mathbf{E}_h$ are thus simply connected by $\widetilde{\mathbf{e}}_i = \widetilde{\mathbf{e}}_{i+n_e} = \mathbf{e}_i$. Vice versa, we can associate to any function $\widetilde{\mathbf{E}}_h \in \widetilde{V}_h$ a function $\mathbf{E}_h = \Pi_h \widetilde{\mathbf{E}}_h \in V_h$ by defining its coordinates as $\mathbf{e}_i = \frac{1}{2}(\widetilde{\mathbf{e}}_i + \widetilde{\mathbf{e}}_{i+n_e})$. In linear algebra notation, this reads

$$\mathbf{e} = \mathrm{P}\,\widetilde{\mathbf{e}}, \tag{16}$$

with projection matrix P defined by $\mathrm{P}_{ij} = \frac{1}{2}$ if $j = i$ or $j = i + n_e$, and $\mathrm{P}_{ij} = 0$ else.

We now define system matrices for the system (3)–(4) by $(\mathrm{M}_\mu)_{ij} = (\mu\psi_j, \psi_i)$, $\mathrm{C}_{ij} = \mathrm{C}'_{ji} = (\operatorname{curl}\phi_j, \psi_i)$, and $\mathrm{M}_\epsilon^{-1} = \mathrm{P}\,\widetilde{\mathrm{M}}_\epsilon^{-1}\mathrm{P}^\top$, where $\widetilde{\mathrm{M}}_\epsilon$ is defined as in the previous sections. This construction has the following properties.

Lemma 3 *Let* M_μ, C, C′, *and* M_ϵ^{-1} *be defined as above, and set* $\mathrm{M}_\epsilon = (\mathrm{M}_\epsilon^{-1})^{-1}$. *Then the conditions (i)–(iii) are satisfied.*

Proof Condition (i) follows by construction. The matrix M_μ is diagonal and positive definite and therefore M_μ^{-1} has the same properties. This verifies (ii) and (iii) for the matrix M_μ. Since P is sparse and has fully rank and $\widetilde{\mathrm{M}}_\epsilon^{-1}$ is block diagonal, symmetric, and positive definite, one can see that also M_ϵ^{-1} is sparse, symmetric, and positive-definite. This verifies conditions (ii) and (iii) for M_ϵ. □

In the following, we investigate more closely the relation of the system (3)–(4) with matrices as defined above and the system (10)–(11) discussed in the previous section. We start with an auxiliary result.

Lemma 4 *Let* C, P, *and* $\widetilde{\mathrm{C}}$ *be defined as above. Then one has* $\widetilde{\mathrm{C}} = \mathrm{CP}$.

Proof The result follows directly from the construction. □

As a direct consequence, we can reveal the following close connection between the methods (3)–(4) and (10)–(11) discussed in the preceding sections.

Lemma 5 *Let* $\widetilde{\mathbf{e}}(t)$, $\widetilde{\mathbf{h}}(t)$ *be a solution of (10)–(11). Then* $\mathbf{e}(t) = \mathrm{P}\widetilde{\mathbf{e}}(t)$, $\mathbf{h}(t) = \widetilde{\mathbf{h}}(t)$ *solves (3)–(4) with matrices* M_ϵ, M_μ, *and* C *as defined above.*

Proof From Eq. (10), the definition of $\mathbf{e}$, $\mathbf{h}$, and Lemma 4, we deduce that

$$\partial_t \mathbf{e} = \mathrm{P}\partial_t \widetilde{\mathbf{e}} = \mathrm{P}\widetilde{\mathrm{M}}_\epsilon^{-1}\widetilde{\mathrm{C}}^\top \widetilde{\mathbf{h}} = \mathrm{P}\widetilde{\mathrm{M}}_\epsilon^{-1}\mathrm{P}^\top \mathrm{C}^\top \widetilde{\mathbf{h}} = \mathrm{M}_\epsilon^{-1}\mathrm{C}^\top \mathbf{h}.$$

This verifies the validity of Eq. (3). Using Eq. (11), we obtain

$$\mathrm{M}_\mu \partial_t \mathbf{h} = \widetilde{\mathrm{M}}_\mu \partial_t \widetilde{\mathbf{h}} = -\widetilde{\mathrm{C}}\,\widetilde{\mathbf{e}} = -\mathrm{CP}\,\widetilde{\mathbf{e}} = -\mathrm{C}\,\mathbf{e},$$

which verifies the validity of Eq. (4). Finally, using the discrete stability of the projection completes the proof. □

Remark 2 The vectors $\mathbf{e}(t)$, $\mathbf{h}(t)$ computed via (3)–(4) with the above choice of matrices correspond to finite element approximations $\mathbf{E}_h(t) \in V_h$, $\mathbf{H}_h(t) \in Q_h$. Therefore, the procedure described above can be interpreted as a mixed finite element method with mass-lumping based on the approximation spaces V_h and Q_h.

As an immediate consequence of Lemma 5 and the approximation results of Lemma 2, we now obtain the following assertions.

Lemma 6 *Let* $\mathbf{e}(t)$, $\mathbf{h}(t)$ *denote the solutions of (3)–(4) with appropriate initial conditions and set* $\mathbf{E}_h(t) = \sum_i \mathbf{e}_i(t)\phi_i$, $\mathbf{H}_h(t) = \sum_j \mathbf{h}_j(t)\psi_j$. *Then*

$$\|\mathbf{E}_h(t) - \mathbf{E}(t)\|_{L^2(\Omega)} + \|\mathbf{H}_h(t) - \mathbf{H}(t)\|_{L^2(\Omega)} \le Ch,$$

for all $0 < t \le T$. *In addition,* $\|\pi_h^0 \mathbf{H}(t) - \mathbf{H}_h(t)\|_{L^2(\Omega)} \le Ch^2$ *where* $\pi_h^0 \mathbf{H}$ *denotes the piecewise constant approximation of* $\mathbf{H}$ *on the mesh* $\mathcal{T}_h$.

By some elementary computations, one can verify the following observation.

Lemma 7 *Let* $\mathcal{T}_h$ *be a uniform mesh consisting of orthogonal quadrilaterals* T *of the same size. Furthermore, let* ϵ *and* μ *be positive constants. Then the matrices* M_ϵ, M_μ, *and* C, *defined above coincide with those obtained by the finite difference approximation on staggered grids; see [3] for the two dimensional version.*

The method proposed in this section therefore can be understood as a variational extension of the Yee scheme in the sense of [3]. In the two dimensional setting, one degree of freedom $\mathbf{e}_i$ is required for every edge, and one value $\mathbf{h}_j$ for every element.

4 Numerical Validation

Consider the domain $\Omega = (-1,1)^2 \setminus \{(x,y) : (x-0.6)^2 + y^2 \leq 0.25^2\}$, which is split by an interior boundary into $\Omega = \Omega_1 \cup \Omega_2$; see Fig. 4 for a sketch. We set $\epsilon = 1$ on Ω_1, $\epsilon = 3$ on Ω_2 and $\mu = 1$ on Ω, and consider a plane wave that enters the domain from the left boundary. The wave gets slowed down and refracted, when entering the domain Ω_2, and reflected at the circle $\partial\Omega_0$, where we enforce a perfect electric boundary conditions. For the spatial discretization, we choose the method presented in Sect. 3, while for the time discretization, we choose the leap-frog scheme. A very small time step is chosen to suppress the additional errors due to time discretization. Convergence rates for the numerical solution are depicted in table of Fig. 5 and a few snapshots of the solution are depicted Fig. 6. The error is measured in the norm $|||e||| := \max_{0\leq t^n\leq T} \|e(t^n)\|_{L^2(\Omega)}$.

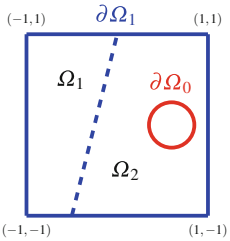

Fig. 4 Geometry

h	DOF	$\|\|\|\mathbf{E}_h - \pi_h\mathbf{E}_{h^*}\|\|\|$	eoc	$\|\|\|\pi_h^0(\mathbf{H}_h - \pi_h\mathbf{H}_{h^*})\|\|\|$	eoc
2^{-3}	2246	0.158291	—	0.242490	—
2^{-4}	8884	0.057465	1.46	0.069676	1.80
2^{-5}	35368	0.025145	1.19	0.017157	2.02
2^{-6}	141136	0.011835	1.08	0.004064	2.07

Fig. 5 Errors and estimated order of convergence (eoc) with respect to a fine solution $(\mathbf{E}_{h^*}, \mathbf{H}_{h^*})$ for $h^* = 2^{-8}$. The total number of degrees of freedom (DOF) is also given

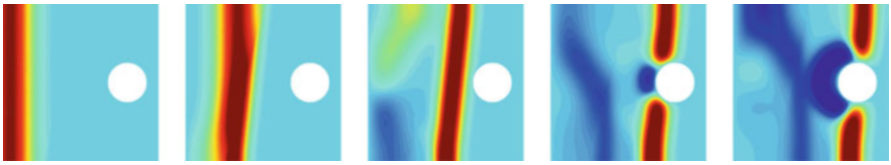

Fig. 6 Snapshots of the magnetic field intensity $\mathbf{H}_h$ for time $t = 0.8, 1.2, 1.6, 2.4, 2.8$

5 Discussion

Before we conclude, let us briefly discuss an alternative formulation and the extension to three dimensions and higher order approximations.

Remark 3 Eliminating $\mathbf{h}$ from (3)–(4) leads to a second order equation

$$\mathrm{M}_\epsilon \, \partial_{tt} \mathbf{e} = \mathrm{K}_{\mu^{-1}} \mathbf{e} \tag{17}$$

for the electric field vector $\mathbf{e}$ alone, with $\mathrm{K}_{\mu^{-1}} = C' \mathrm{M}_\mu^{-1} \mathrm{C}$. A sufficient condition for the stability of the scheme (17) is

(iv) M_ϵ and $\mathrm{K}_{\mu^{-1}}$ are symmetric and positive definite, respectively, semi-definite,

and for an efficient numerical integration of (17), one now requires that

(v) M_ϵ^{-1} and $\mathrm{K}_{\mu^{-1}}$ can be applied efficiently.

The conditions (iv) and (v) can be seen to be a direct consequence of the conditions (i)–(iii), and the special form $\mathrm{K}_{\mu^{-1}} = \mathrm{C}' \mathrm{M}_\mu^{-1} \mathrm{C}$ of the matrix $\mathrm{K}_{\mu^{-1}}$.

Remark 4 Using the definition of the matrices M_μ, C, and $\mathrm{C}' = \mathrm{C}^\top$ given in the previous section, one can verify that $\mathrm{K}_{\mu^{-1}}$ is given by $(\mathrm{K}_{\mu^{-1}})_{ij} = (\mu^{-1} \operatorname{curl} \phi_j, \operatorname{curl} \phi_i)$. Thus $\mathrm{K}_{\mu^{-1}}$ can be assembled without constructing C or M_μ explicitly. Moreover, the conditions (iv) and (v) for $\mathrm{K}_{\mu^{-1}}$ are satisfied automatically. The essential ingredient for a mass-lumped mixed finite element approximation of (1)–(2) thus is the construction of a positive definite and sparse matrix M_ϵ^{-1}.

Remark 5 The construction of the approximation M_ϵ discussed in Sect. 3 immediately generalizes to three space dimensions. Like in the two dimensional case, two basis functions $\widetilde{\phi}_i$, $\widetilde{\phi}_{i+n_e}$ of the space $\widetilde{V}_h$ are defined for every edge e_i of the mesh [9, 10] and the approximation $(\cdot, \cdot)_h$ is defined via numerical quadrature by the vertex rule. The lumped mass matrix given by $(\widetilde{\mathrm{M}}_\epsilon)_{ij} = (\epsilon \widetilde{\phi}_j, \widetilde{\phi}_i)_h$ then is again block-diagonal. As before, the basis functions for the space V_h are then defined by $\phi_i = \widetilde{\phi}_i + \widetilde{\phi}_{i+n_e}$ and the inverse mass matrix for the reduced space is again given by $\mathrm{M}_\epsilon^{-1} = \mathrm{P} \, \widetilde{\mathrm{M}}_\epsilon^{-1} \mathrm{P}^\top$ with projection matrix P of the same form as in two dimensions.

Acknowledgments The authors are grateful for support by the German Research Foundation (DFG) via grants TRR 146, TRR 154, and Eg-331/1-1 and through grant GSC 233 of the "Excellence Initiative" of the German Federal and State Governments.

References

1. Boffi, D., Brezzi, F., Fortin, M.: Mixed Finite Element Methods and Applications. Springer Series in Computational Mathematics, vol. 44. Springer, Heidelberg (2013)
2. Codecasa, L., Politi, M.: Explicit, consistent, and conditionally stable extension of FD-TD to tetrahedral grids by FIT. IEEE Trans. Magn. **44**, 1258–1261 (2008)

3. Cohen, G.: Higher-Order Numerical Methods for Transient Wave Equations. Springer, Heidelberg (2002)
4. Cohen, G., Monk, P.: Gauss point mass lumping schemes for Maxwell's equations. Numer. Methods Partial Diff. Equat. **14**, 63–88 (1998)
5. Egger, H., Radu, B.: A mass-lumped mixed finite element method for acoustic wave propagation (2018). arXive:1803.04238
6. Elmkies, A., Joly, P.: éléments finis d'arête et condensation de masse pour les équations de Maxwell: le cas de dimension 3. C. R. Acad. Sci. Paris Sér. I Math. **325**, 1217–1222 (1997)
7. Joly, P.: Variational methods for time-dependent wave propagation problems. In: Topics in Computational Wave Propagation, LNCSE, vol. 31, pp. 201–264. Springer, Berlin (2003)
8. Monk, P.: Analysis of a finite element methods for Maxwell's equations. SIAM J. Numer. Anal. **29**, 714–729 (1992)
9. Mur, G., de Hoop, A.T.: A finite-element method for computing three-dimensional electromagnetic fields in inhomogeneous media. IEEE Trans. Magn. **21**(6), 2188–2191 (1985)
10. Nedelec, J.C. : Mixed finite elements in $\mathbb{R}^3$. Numer. Math. **35**(6), 315–341 (1980)
11. Schuhmann, R., Weiland, T.: A stable interpolation technique for FDTD on non-orthogonal grids. Int. J. Numer. Model. **11**, 299–306 (1998)
12. Weiland, T.: Time domain electromagnetic field computation with finite difference methods. Int. J. Numer. Model. **9**, 295–319 (1996)
13. Yee, K.: Numerical solution of initial boundary value problems involving Maxwell's equations in isotropic media. IEEE Trans. Antennas Propag. **AP-16**, 302–307 (1966)